Confined strength and deformation of second-year columnar-grained sea ice in Mould Bay

Sinha, N. K.

Publisher's version / Version de l'éditeur:

Proceedings of the Fourth International Offshore Mechanics and Arctic Engineering Symposium, 2, pp. 209-219, 1985-02-10

National Research Council Canada
Conseil national de recherches Canada

CONFINED STRENGTH AND DEFORMATION OF SECOND–YEAR COLUMNAR–GRAINED SEA ICE IN MOULD BAY

by N.K. Sinha

Reprinted from
Proceedings of the Fourth International Offshore
Mechanics and Arctic Engineering Symposium, ASME
Dallas, Texas, February 10 - 15, 1985
Volume II, p. 209 - 219

DBR Paper No. 1286
Division of Building Research

Price $1.00 OTTAWA NRCC 24497

Canada

RÉSUMÉ

On a procédé dans la région extrême nord de l'Arctique à des essais in situ de compression sous étreinte latérale, sur de la glace de mer à grains columnaires de deuxième année de texture et structure orthotropiques. La charge et la contrainte latérale ont été appliquées dans un plan perpendiculaire au grand axe des grains columnaires. Les charges axiales et de contrainte latérale on été mesurées en même temps que les déformations axiales et latérales. En imposant une étreinte latérale, on augmente considérablement la résistance mécanique, mais on réduit de façon significative le coefficient de sensibilité de la résistance. On a constaté que la résistance de cette glace de mer en présence d'une étreinte latérale était comparable à celle d'échantillons de glace d'eau douce à grains columnaires fabriquée en laboratoire et soumise aux essais dans des conditions idéales. L'étude a démontré qu'il était possible d'effectuer in situ des études fiables et élaborées de la résistance.

CONFINED STRENGTH AND DEFORMATION OF SECOND-YEAR COLUMNAR-GRAINED SEA ICE IN MOULD BAY

N. K. Sinha
Division of Building Research
National Research Council of Canada
Ottawa, Ontario, Canada

ABSTRACT

Second-year columnar-grained sea ice with orthotropic texture and fabric has been tested in the field in the High Arctic under confined compressive loading conditions. Both load and confinement were applied in the plane at right angles to the long axis of the columnar grains. Axial and confining loads were measured along with the measurements of axial and lateral strains. The confinement increases the strength considerably but significantly decreases the rate sensitivity of strength. The confined strength of this sea ice has been found to be comparable to the confined strength of laboratory-made fresh water columnar-grained ice tested under ideal conditions. The investigation showed that reliable and fairly sophisticated strength studies can also be carried out in the field.

INTRODUCTION

Mould Bay, Prince Patrick Island, N.W.T., Canada proved to be an ideal study site for investigations related to the aging of Arctic sea ice (Sinha, 1983a; 1984; Holt and Digby, 1984; Troy et al, 1984; Digby, 1984). The ice cover that formed in the 1981-82 growth season survived the summer melt season of 1982 and remained essentially intact in the bay, then went through a second growth season in the winter of 1982-83. Detailed documentation of the physical, chemical and microwave properties of the ice was carried out four times: in October 1981, in June-July 1982, in April-May 1983 and in March-April 1984. The weather conditions, ice thickness and snow thickness were monitored on an almost continuous basis. The High Arctic Weather Station (76°N; 119°20'W) situated on the eastern shore of Mould Bay was used as the base camp for a Canadian multi-departmental joint investigation known as the Radarsat Project.

During the field trip of April-May 1983, observations were made on rate sensitivity of uniaxial unconfined and confined compressive strength and deformation of columnar-grained ice in the bay. This paper describes results obtained on the confined compressive strength of the ice with both load and confinement applied in the plane of the ice cover, i.e., perpendicular to the columns. The paper also brings out the numerous problems that were encountered during field tests.

ICE CHARACTERISTICS

Mould Bay, which is about 30 km long and more than 10 km wide at some locations, was covered with an extremely uniform flat sheet of new ice during the 1981-82 growth season. Detailed descriptions of the young sea ice cover of October 1981, including a SLAR (Side Looking Airborne Radar) image, has been given in Sinha (1984). The thickness of the ice cover during the 3rd week of October 1981 was 0.4 ± 0.05 m. Examination of the ice at the various stations established along an east-west experimental line showed a predominantly columnar-grained structure except for the ice cover near the eastern shore that consisted almost entirely of congealed, frazil slush type ice. This ice cover stayed intact and grew to a total thickness of 2.0 ± 0.20 m at the end of the growth season. Reexamination in June-July 1982 revealed that the ice was columnar-grained through the entire depth of the ice cover. During the summer of 1982 considerable melting of the ice cover occurred, and several leads formed across the bay. However, the ice cover as a whole survived, except near the shore lines, and entered the new growth period of 1982-83. Measurements carried out during the April-May 1983 trip revealed that the thickness of the second-year ice on top of the new ice was less than a metre.

For the tests to be reported here, ice was obtained from Station #3, about 2 km from the eastern shore. The total ice thickness at this site was 1.87 m on April 9, 1983. Samples were obtained during previous strength tests on young ice at essentially the same location in October 1981 (Sinha, 1984) and on mature first-year ice in June-July (Sinha, 1983a). Vertical cores of 76 mm diameter and full depth of the ice cover were obtained for microstructural and salinity analysis. Large blocks of ice cut with a chain saw were obtained for strength tests. The air temperature during this trip ranged from -46°C to -20°C. Ice samples were usually wrapped with insulation and shock-absorbing materials soon after recovery to prevent damage from sudden temperature changes during the return trip to the base camp.

The density profile given by curve 'a' of Figure 1 was obtained by slicing the 0.1 m wide and 0.04 m thick vertical block shown in the photograph. Although the top layer of the ice was very porous, the density increased rapidly with depth. For this reason the top 0.05 m of the ice was discarded when specimens for strength tests were prepared. Curve 'b' shows the density obtained from the mass and volume of a set of samples used for determining the strength. The average density of the ice (obtained from 16 specimens tested) was found to be 910.3 ± 4.1 $kg \cdot m^{-3}$ (air volume of 8.2 ± 4.5 ‰) at -10°C; the highest and the lowest were 915.9 $kg \cdot m^{-3}$ and 905.0 $kg \cdot m^{-3}$ respectively. The air volume was estimated using 917.8 $kg \cdot m^{-3}$ as the density of pure ice at -10°C.

The ice was columnar-grained through its entire depth, including the old ice/new ice interface, the mean c-axis of the grains tending to be in the horizontal plane (±5°), parallel to the surface of the ice cover (Figure 2). The mean c-axis of the grains in the horizontal plane (see Figure 2) tended to be parallel (±15°) to the axis of the channel or the bay, similar to previous observations in Mould Bay (Sinha, 1983a; 1984). This type of anisotropy in the fabric of columnar-grained ice is quite common (Weeks and Gow 1978; 1980; Sinha, 1983b; Nakawo and Sinha, 1984). The present observations indicate that the aging processes that led to the complete desalination in the old ice did not affect the texture and the fabric of the ice. In fact, even the air porosity is comparable to that obtained directly by Nakawo (1983) in first year ice grown under similar growth rate as this ice cover. The ice cover did not appear to rotate in the bay during the melt season more than the experimental uncertainty (5 to 10°) of marking the orientation of the axis of the bay on a block of ice.

Figure 2b shows that it is difficult to define a grain, let alone determine a representative grain size. The ice could best be described in terms of families of sub-grains lined up with their c-axis oriented in a general direction. The bubbles are very irregular in shape (Figure 1) and they are present at the sub-grain boundaries as shown in Figure 2c. The sub-grain boundaries in the micrographs were developed by a microtoming and etching technique described earlier (Sinha, 1977). The microstructural examinations were performed in the field soon after recovery of the samples.

Since the ice was orthotropic in texture as well as in fabric, the coordinates x_1 and x_2 were chosen in the plane of the ice cover (horizontal plane) and x_3 parallel to the axis of the columnar grains (in the vertical plane). Furthermore it was decided, for simplicity, to make x_1 parallel to the mean c-axis or [0001] axis orientation of the grains. Rectangular specimens for testing were prepared with their major axes (along which load was also applied) at angles α and γ with x_1 and x_3 respectively. Consequently orientation of the axial load with respect to the ice cover, hence the c-axis, is described by the angles α and γ. The present report concerns only horizontally-oriented samples (γ = 90°).

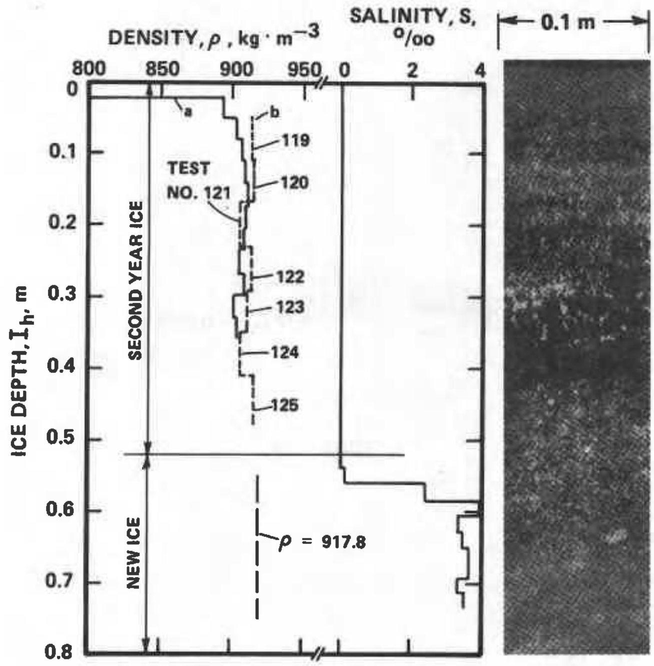

FIG. 1 Vertical density and salinity profile in second-year sea ice at Station 3 in Mould Bay, April 1983.

EXPERIMENTAL METHODS

The tests were conducted in a mobile trailer at -10 ± 0.5°C. Surface temperatures of the specimens were measured both before and after testing, using a thermistor system.

Tests were carried out on large prismatic samples with dimensions of 50 × 101 × 250 mm, their long dimensions parallel to the surface of the ice cover (γ = 90°). Two types of specimens were prepared with α = 0° and α = 45°. A portable band saw kept inside the cold room at -10°C was used to prepare the samples. The specimen surfaces were finished by hand with medium grade sandpaper on a flat surface. The top and bottom end surfaces (50 × 101 mm) and the two side faces (50 × 250 mm) were prepared manually, as carefully as possible to make certain that they were flat and at right angles to the 101 × 250 faces. Final finish was given by wiping with a tissue paper slightly moistened with alcohol. Finished specimens were weighed inside the cold room, with a balance capable of measuring to an accuracy of 0.01 gm, and their dimensions measured with a vernier calipers. On the average, the specimens' final dimensions did not vary from the desired size by more than 0.2 mm. (The best was 0.05 mm but the worst was 0.45 mm.) Each specimen was photographed and stored separately in a plastic bag from which the air was sucked out as much as possible.

The test specimens were prepared from three large blocks, approximately 200 × 400 mm in the horizontal plane and about 800 mm deep, covering the full depth of the second-year ice. After discarding the top porous 50 mm of the ice and the new ice at the bottom, each block provided sufficient depth for seven specimens. Although crystallographically the samples from the same block were very similar, the bubble structures varied greatly because of layering. This is illustrated by the photographs of finished specimens numbered 119 to 125 presented in Figure 3. Each photograph is of the top horizontal surface of the samples with respect to their original position in the ice cover. Because of

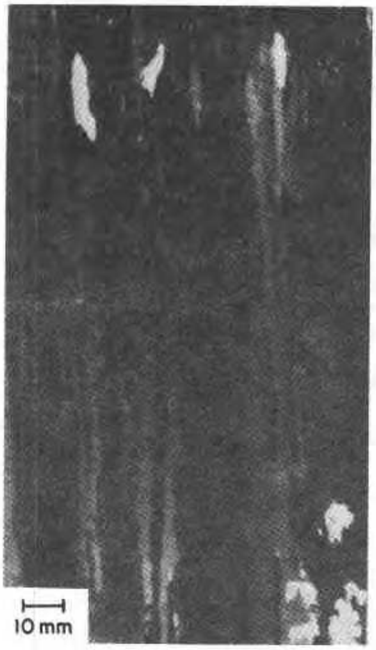

FIG. 2a Vertical section showing columnar grains.

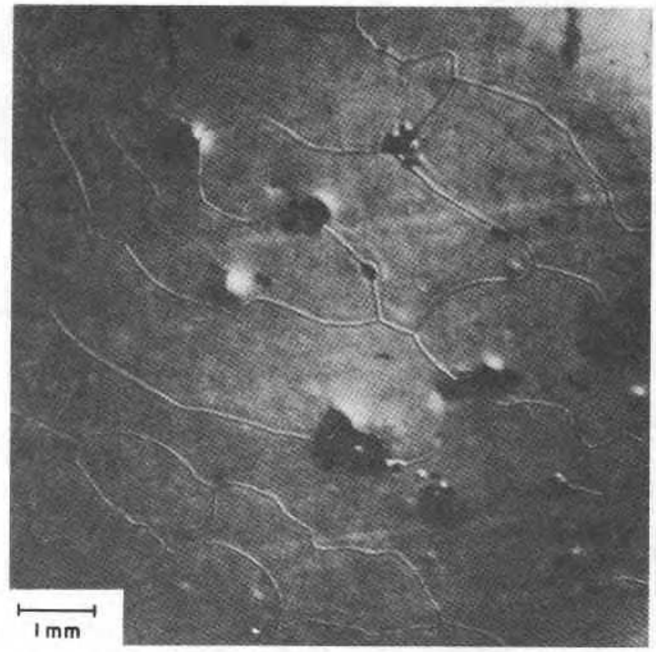

FIG. 2c Optical micrograph of an etched horizontal section showing the oriented subgrains and cross-sections of irregularly-shaped air bubbles.

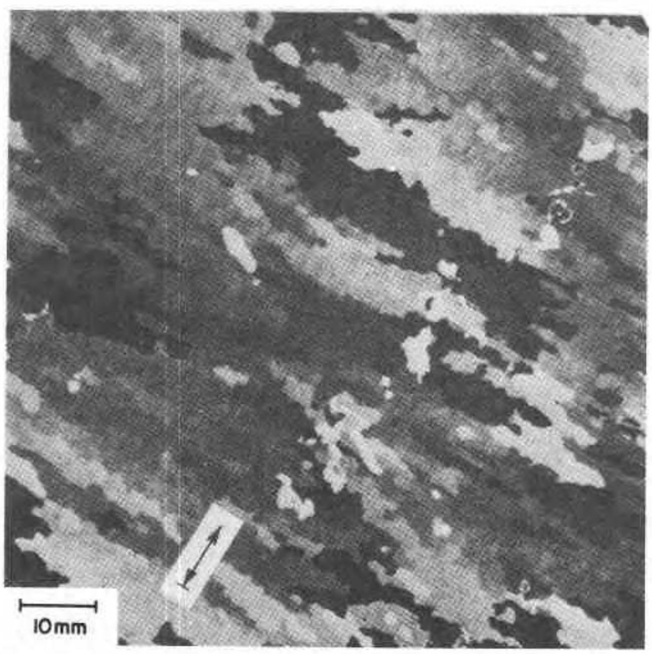

FIG. 2b Horizontal thin section at a depth of 368 mm from the surface. The arrow indicates the long axis of Mould Bay.

the layer variation in bubble concentration, the density varied from sample to sample. The seven samples presented in Figure 3 were oriented with $\alpha = 45°$ and their densities are given by curve 'b' in Figure 1. Note the crack orientations after the test.

A commercial test machine (Soiltest CT-405) with a design load capacity of 50 kN was used to perform the tests (Figure 4). It is a conventional screw-driven machine capable of delivering a constant actuator displacement rate, $\dot{x}_1$, up to 7×10^{-2} mm s^{-1}, or a nominal strain rate, $\dot{\varepsilon}_{1n} = \dot{x}_1/\ell$, up to 2.8×10^{-4} s^{-1} for a specimen length, ℓ, of 250 mm. Each specimen was tested between a pair of 25 mm thick polished aluminum subplatens having planer dimensions of 60 × 100 mm with load applied in the x_1 direction across the 50 × 101 mm faces. The top subplatens reacted against the test frame through a calibrated load cell. The bottom subplaten was supported by a polished 150 mm steel platen, normally used for unconfined tests, attached to the actuator. Note that the subplatens are 1 mm shorter than the specimen width. This provided a 0.5 mm clearance on either side between the subplatens and the confining platens. The stress, σ_1, was estimated from the axial loads and the areas of the end surfaces of the specimens. Axial specimen deformation was measured with a pair of specially designed gauges, of 150 mm in gauge length (Sinha, 1981), mounted directly on the central areas of the two 101 × 250 mm faces of the specimen.

A specially-designed subpress (Figure 4) was used to apply confinement across the 50 × 250 mm faces, i.e. along the x_2 direction. This was accomplished by a pair of 25 mm thick aluminum platens. One of these platens was fixed to the subpress frame, consisting of six stainless steel solid rods of 32 mm diameter. The other platen was centrally attached to a movable 51 mm

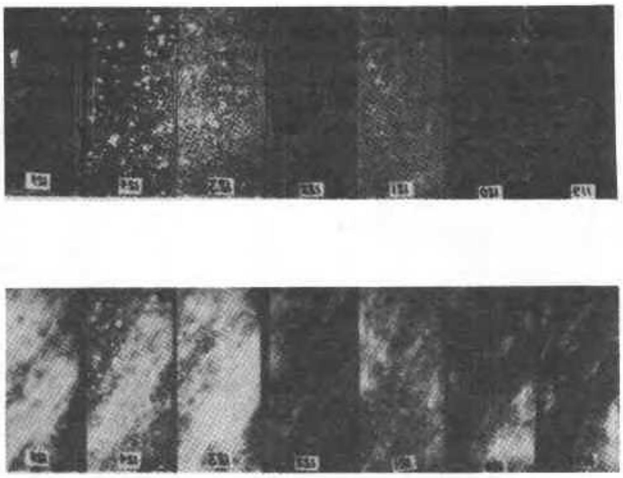

FIG. 3 A set of specimens with $\alpha = 45°$ and $\gamma = 90°$ photographed before (top row) and after (bottom row) the tests.

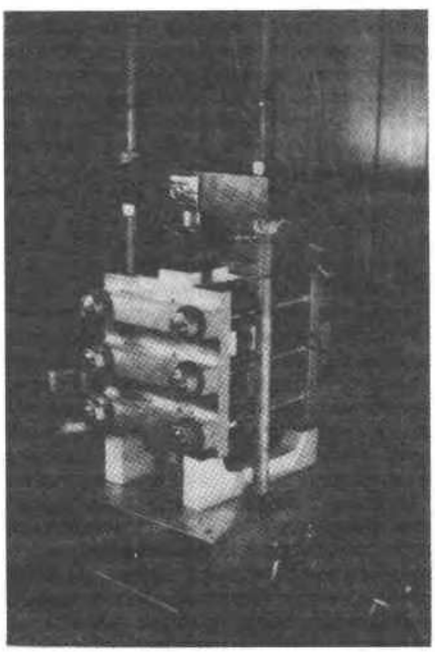

FIG. 4 Test machine and the confining frame photographed during a test in the field.

diameter threaded stainless steel rod and reacted against the frame through a calibrated load cell and a threaded locking mechanism. This arrangement was essential for moving the platen back and forth for final adjustments to ensure a good initial contact with the 50 × 250 mm faces, contact being ensured by a preload of about 0.05 $MN \cdot m^{-2}$. The subpress was designed to keep the side platens parallel to each other during testing. In order to ensure that the lateral deformation was symmetric about the axis of loading, the entire subpress was installed on a carriage, as can be seen in Figure 4, capable of moving freely in the lateral direction during testing. A pair of displacement gauges were mounted between the two side platens to record the lateral deformation. Output from the two load cells and the four displacement gauges was recorded separately using strip chart recorders and a magnetic tape with a digital data logging system capable of working at subzero temperatures. The chart recorders were kept in heated and well insulated boxes that also housed the load cell electronics and the power supply for the DCDTs (direct current displacement transducer) of the displacement gauges. Calibration of these gauges was checked after every few tests to ensure the accuracy of the strain measurements. A polyethylene sheet of 0.15 mm was stretched on each confining platen to reduce friction on the confining sides of the subpress (Frederking, 1977).

RESULTS AND ANALYSIS

Early in the test series it became clear that the ice was stronger than anticipated. Therefore, the maximum load level would exceed the machine's design capacity for nominal strain rates greater than 1×10^{-5} s^{-1} though it is capable of operating at a nominal strain rate of 2.8×10^{-4} s^{-1} (Sinha, 1984). Based on previous experience (Sinha, 1983a) it was decided not to exceed the machine capacity by more than about 150%, in other words a total load level of 75 kN. The operating range was decreased to a maximum nominal rate of about 5×10^{-5} s^{-1}. The machine started slipping and failing to turn the loading screw when the total load exceeded about 35 kN for rates less than 5×10^{-6} s^{-1}. This problem had not been experienced previously and examination showed that it was caused by the test machine's design. Experimental rates were therefore limited by these boundaries and all the failures were noted to be of the upper yield type as defined and discussed in detail in Sinha (1981).

An example of axial stress, σ_1, and the corresponding strain, ε_1, for a confined test at a nominal rate of 4.4×10^{-5} s^{-1} is shown in Figures 5a and 5b respectively. In this case the specimen was unloaded soon after reaching the upper yield or failure stress, σ_{1f}, of 14.8 $MN \cdot m^{-2}$ at a failure time, t_f, of 315 seconds. Note that the total load on the specimen exceeded the design capacity of the machine halfway to failure time. It can be seen that the strain rate in the specimen increased rapidly for about 110 seconds and thereafter increased very slowly, practically constant and equal to the nominal rate. This can be seen from the broken line corresponding to the constant, $\dot{\varepsilon}_n$. The major transition in the strain rate occurred after the load level exceeded about half the design capacity of the machine. The average axial strain rate to failure, $\dot{\varepsilon}_{1af} = \varepsilon_{1f}/t_f$, where ε_{1f} is the axial strain at upper yield, was comparable but somewhat less (10%) than $\dot{\varepsilon}_n$. This observation sharply contrasts with the measurements carried out on ice in uniaxial unconfined loading under truly constant cross-head rates (Sinha, 1981; 1984). For constant cross-head rates, the average strain rates were found to be a fraction of the nominal rate. However, measurements by the author (unpublished) during closed-loop controlled constant strain rate experiments with the controlling gauge mounted directly on the specimen, indicated that the cross-head rate should indeed decrease, instead of being constant, during the pre-upper-yield period to maintain a constant deformation rate in the specimen. This observation indicates, therefore, that the machine could not maintain a constant cross-head rate during the later part of the test in Figure 5. No measurements of the

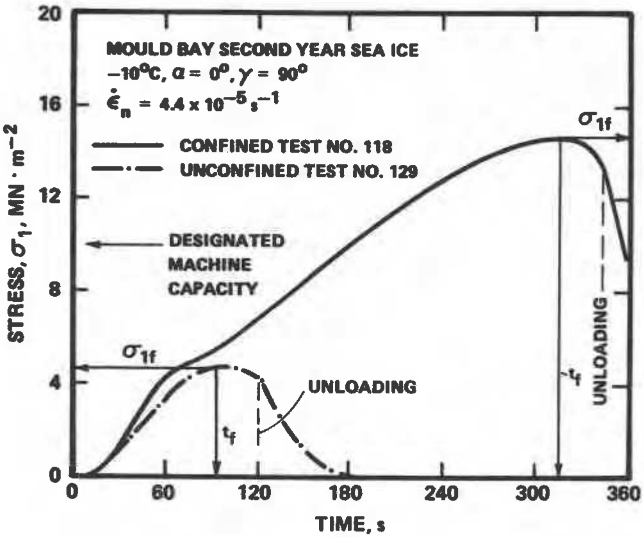

FIG. 5a Stress history for a confined and an unconfined test at the same cross-head displacement rate.

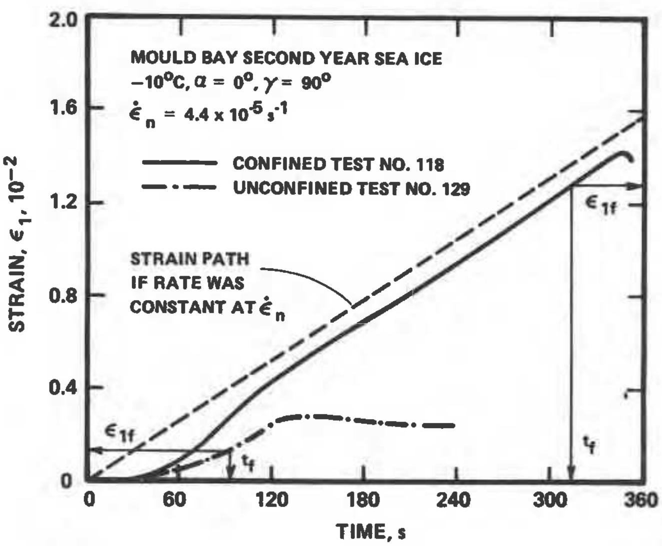

FIG. 5b Strain history for these tests.

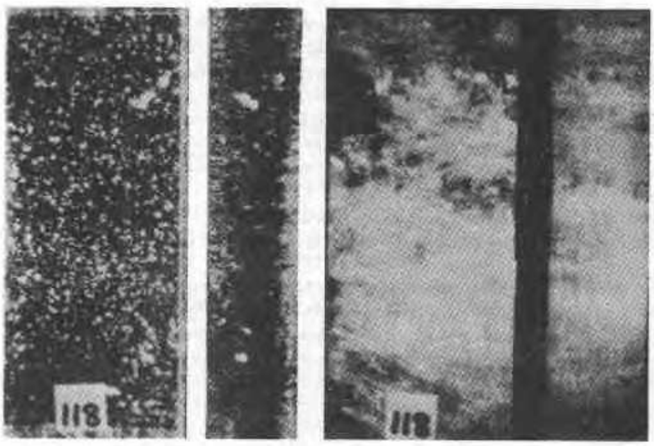

FIG. 5c Front and side views of specimen No. 118 before (left) and after (right) test. Note the cracks in the front view and the irregularities in the side view after test.

cross-head rates during these tests were made to substantiate this statement, but a previous test series (Sinha, 1983a) with this machine involving high loads on vertically oriented ($\gamma = 0$) samples of first-year ice from the same location lends some support.

The example shown in Figure 5 represents the worst case in the present series. The purpose of presenting this experiment is to bring out some common problems, as dicussed above, that may be overlooked. Moreover, it also demonstrates a critical experimental problem involving confinement, which is common (Blanchet and Hamza, 1983; Timco and Frederking, 1983). This concerns the quality of specimen preparation and is indicated by the $\sigma_1 - t$ curve exhibiting a hump at about 70 seconds. This hump was thought to be caused by imperfections in the specimen geometry causing imperfect contact between the specimen sides and the confining platens at the beginning of the test. Examination of the pre-test dimensions of the specimen of Figure 5 showed that it had the worst dimensional variations of all the specimens tested in this series. The width of this sample near the top and the bottom was 101.50 mm and 101.55 mm respectively but was 101.10 mm in the central area. It is therefore highly possible that the quality of confinement was less than desired, particularly in the central area, in the beginning and the loading was more like an unconfined situation until the lateral deformation in the specimen resulted in better contact. To test this hypothesis, a comparison was made with the unconfined loading results obtained on a second-year sea ice specimen of similar orientation, from Station #3, at the same nominal rate. It can be seen in Figures 5a and 5b that both the unconfined and the confined tests essentially followed the same stress or deformation history during the initial loading period for about 30 seconds. Note the timing and the stress level of the upper yield point in the unconfined tests and of the stress hump in the confined test. It should perhaps be mentioned here that the strain rate continually varied during the pre-failure time in the unconfined test and that the average strain rate to the upper yield point is about one third of the nominal rate similar to previous observations in laboratory tests (Sinha, 1981). The differences in the failure stresses and strains in the two tests are also particularly noticeable. The maximum stress in the confined test is about three times the corresponding stress in unconfined tests but the failure strain in the former is almost one order of magnitude larger than in the latter.

Figure 6 presents a complete set of results of a test carried out at a nominal rate of 1.7×10^{-5} s^{-1}. In contrast to the previous example, the strain rate varied continuously through the entire test, yielding an average rate equal to about half of $\dot{\varepsilon}_n$. Results shown in Figures 5 and 6 demonstrate that $\dot{\varepsilon}_n$ cannot be used for any serious investigation, although it is still practiced commonly. It is planned to present elsewhere a detailed study on the subject of nominal strain rates and the corresponding actual strain rates under confined and unconfined tests on first year, second year and multi-year ice samples. The stress and strain responses measured during unloading and after complete removal of the axial load (Figure 6) are particularly interesting. Note the quick recovery of the axial strain soon after unloading in the axial direction and the emergence of a residual lateral stress which then relaxed very slowly.

FAILURE STRESS AND TIME

Figure 7 shows that σ_{1f} increases with the decrease in t_f and that the value of α for the specimen has no effect on this dependence. The dependence of σ_{1f} on t_f may be given by

$$\frac{t_f}{t_o} = C\left[\frac{\sigma_{1f}}{\sigma_o}\right]^{-\theta} \qquad (1)$$

where t_o is the unit or reference time (= 1 s) and σ_o is the unit or reference stress (= 1MN$\cdot$m^{-2}). Regression analysis of all the results gave $C = 2.16 \times 10^6$ and $\theta = 3.31$ with a correlation coefficient of 0.81. The numerical value of the stress exponent θ obtained here is greater than the corresponding value, 2.48, obtained under unconfined loading conditions ($\alpha = 0°$, $\gamma = 90°$) for the young sea ice cover at the same location in October 1981 using the same test machine (Sinha, 1984) and a value of 2.57 obtained for unconfined tests on mature first-year ice in the eastern Arctic (Sinha, 1983b) using a very small machine and horizontal samples ($\gamma = 90°$) with $\alpha = 0°$ and 90°.

STRESS-RATE DEPENDENCE

Since strength of ice is sensitive to rate of loading, and since load, hence stress for small strain, and time can be measured easily and accurately without much additional effort, it was shown (Sinha, 1981; 1983a; 1983b; 1984) that the simplest evaluation of the rate sensitivity of strength is obtained by the average stress rate, defined as

$$\frac{\dot{\sigma}_{1af}}{\dot{\sigma}_o} = \frac{\sigma_{1f}/t_f}{\sigma_o/t_o} = \frac{\sigma_{1f}/\sigma_o}{t_f/t_o} \qquad (2)$$

where $\dot{\sigma}_o = \frac{\sigma_o}{t_o}$ is the unit stress rate (= 1 MN$\cdot$m^{-2} s^{-1}).

Substituting t_f/t_o from (1) in (2) and rearranging gives

$$\frac{\sigma_{1f}}{\sigma_o} = C^{\frac{1}{1+\theta}}\left[\frac{\dot{\sigma}_{1af}}{\dot{\sigma}_o}\right]^{\frac{1}{1+\theta}} = 29.49\,(\dot{\sigma}_{1af})^{0.23} \qquad (3)$$

with the values of C and θ, determined earlier. The results are shown in Figure 8.

The dependence of the unconfined upper yield stress on average stress rate for the same ice in Mould Bay when it was only one month old and had a salinity of 5‰, tested with the same machine and orientation, $\gamma = 90°$, $\alpha = 0°$ (Sinha, 1984) is also shown in Figure 8 along with unconfined results obtained on transversely isotropic, fresh water columnar-grained, S-2 ice with load applied, under constant cross-head rates, at right angles to the axis of the columns. These results show clearly the effect of confinement on the rate sensitivity of strength as measured by the stress-rate exponent. Note the significant difference between the stress-rate exponent (0.23) for the confined tests on second-year ice and for the unconfined tests (0.30) on pure fresh water (distilled) ice. Note also that there is practically no difference between the stress rate exponent (0.30) for the fresh water ice and young sea ice (0.29). The presence of brine does not appear to affect the rate sensitivity but the loading boundary condition does.

If S-2 ice is used as the basis for comparison, then Figure 8 shows that the confined strength of second-year sea ice is 3.5 times greater than the unconfined strength of pure ice, when the stress rate is 1×10^{-2} MN$\cdot$m^{-2} s^{-1}, which is about the middle of the experimental range of loading rates.

STRAIN-RATE DEPENDENCE

For the present test series, the average strain rate method was deemed preferable (as discussed in Sinha, 1982; 1983b). The dependence of axial upper yield stress, σ_{1f}, on the average axial strain rate, $\dot{\varepsilon}_{1af} = \varepsilon_{1f}/t_f$, where ε_{1f} is the strain at upper yield, is shown in Figure 9. Again the angle α for the specimen appears to have no effect on strength. The strain rate dependence may be represented by

$$\frac{\sigma_{1f}}{\sigma_o} = P\left[\frac{\dot{\varepsilon}_{1af}}{\dot{\varepsilon}_o}\right]^p \qquad (4)$$

where $\dot{\varepsilon}_o$ is the unit or reference strain rate (= 1 s^{-1}). Regression analysis of all the results gave $P = 81.9$ and $p = 0.18 \pm 0.03$ with a correlation coefficient of 0.84.

The line of best fit given by Equation (4) is shown in Figure 9 along with that for the unconfined results obtained in October 1981 (Sinha, 1984). It also shows two sets of unconfined results on laboratory-made columnar-grained S-2 ice made from distilled water. These sets, because of the purity of the ice and test conditions, could be used as the benchmark for the present study. One set was obtained with a conventional machine with constant cross-head rates and analyzed on the basis of $\dot{\varepsilon}_{1af}$ (Sinha, 1981) and the other set obtained with a closed-loop machine at 'truly' constant strain rates with the controlling displacement gauge mounted directly on the specimens (Sinha, 1982) and failure strain less than about 1×10^{-3}. As in the case of stress-rate analysis, it can be seen here that the rate sensitivity given by the strain rate exponent is essentially the same for both saline and fresh water ice for unconfined tests but is significantly lower in the case of confined tests.

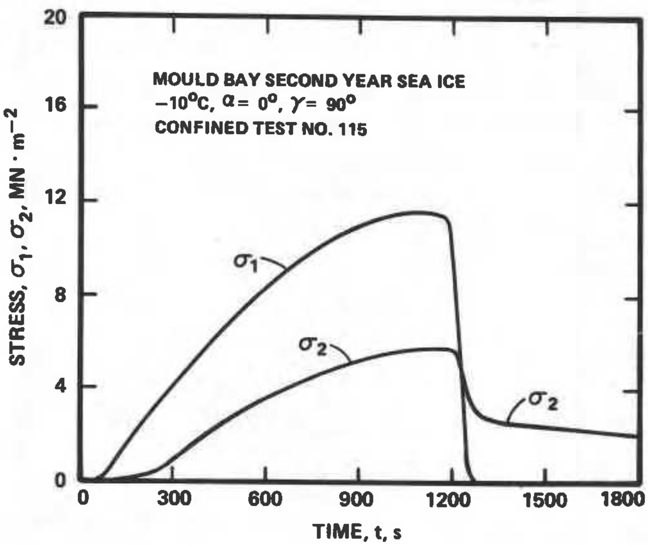

FIG. 6a Axial and lateral stress history for a confined test.

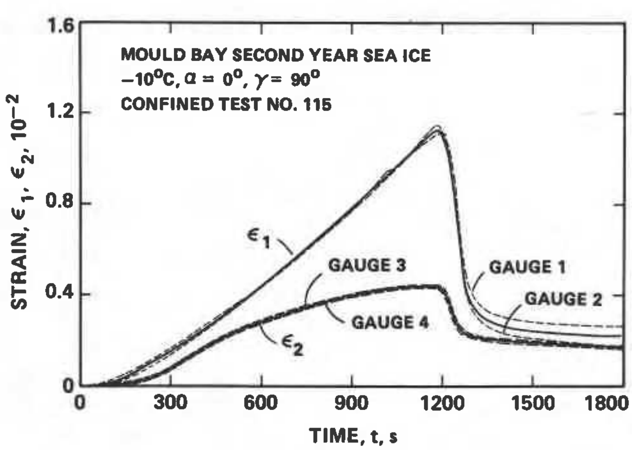

FIG. 6b Axial and lateral strain history for the same test.

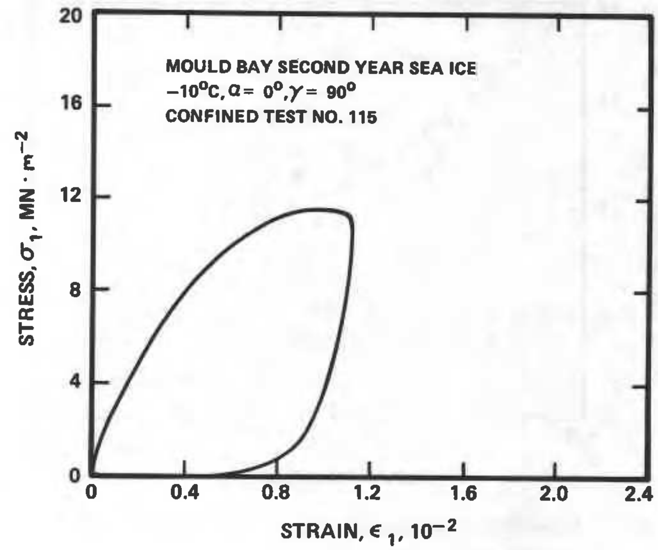

FIG. 6c Stress-strain diagram for the same test

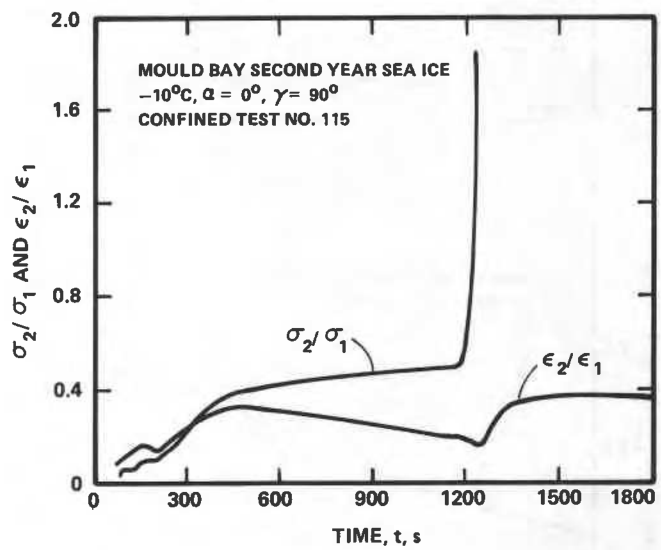

FIG. 6d History of stress and strain ratio for the same test.

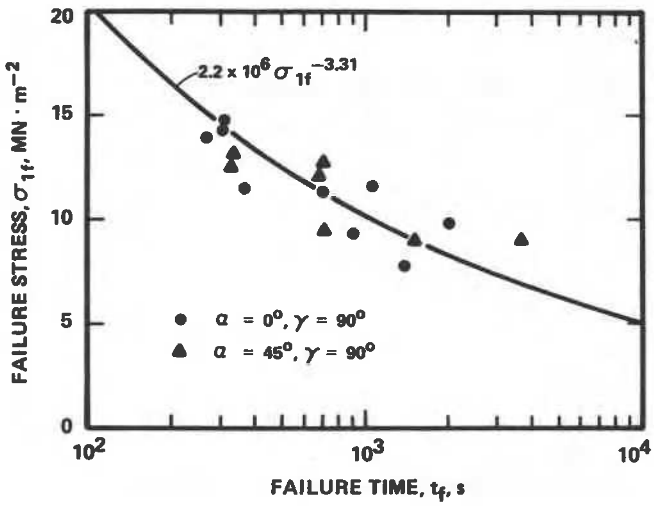

FIG. 7 Dependence of upper axial yield or failure stress on failure time.

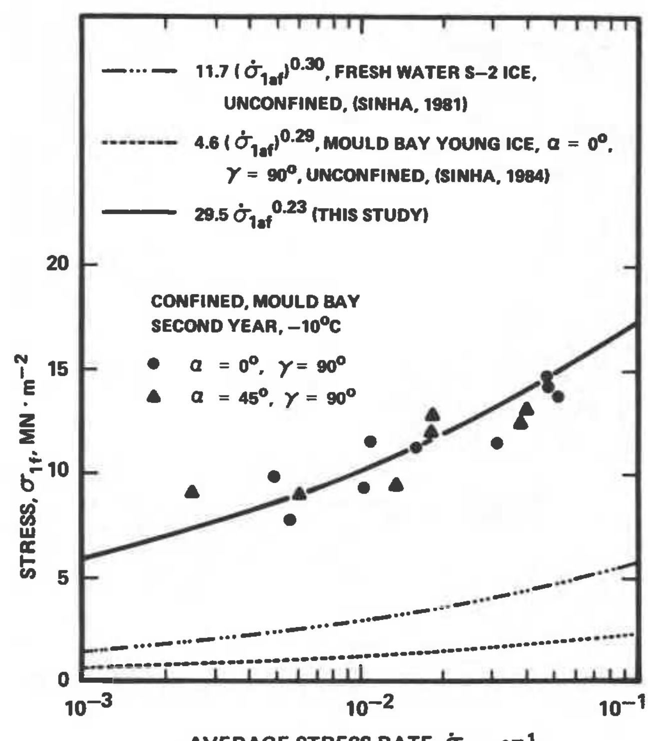

FIG. 8 Dependence of upper axial yield or failure stress on average stress rate.

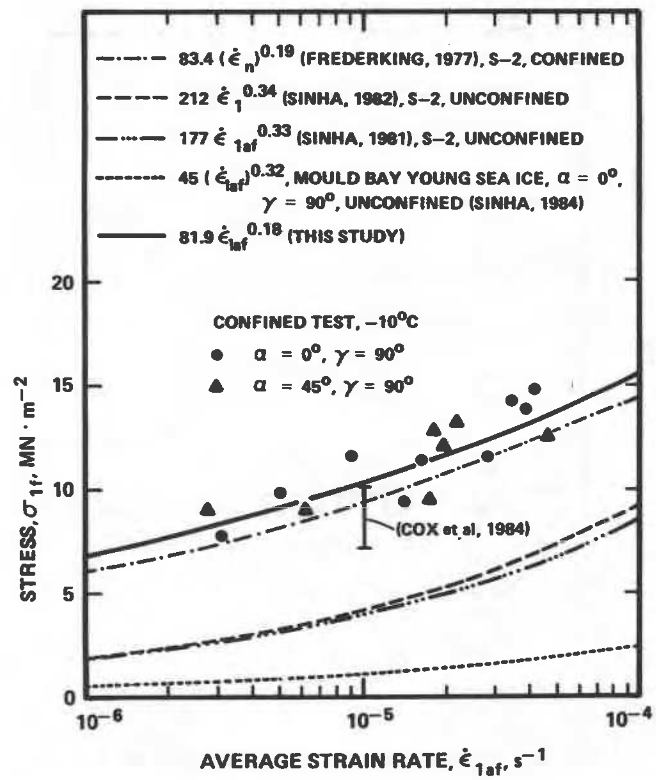

FIG. 9 Dependence of axial upper yield or failure stress on average strain rate.

In the middle of the experimental range of strain rates, at 1×10^{-5} s^{-1}, the ratio of the confined to the unconfined strength is 2.5. This ratio decreases to 1.8 at 1×10^{-4} s^{-1} and increases to 3.6 at 1×10^{-6}. These ratios are significantly lower than the values indicated by the stress-rate analysis described earlier using the same data as in the case of the benchmark.

There are no published data that can be compared directly, without any ambiguity, with the confined test results obtained here. The closest information is that obtained on laboratory-made fresh water transversely-isotropic S-2 ice at -10°C under constant cross-head rates by Frederking (1977), who analysed the results on the basis of nominal strain rates rather than the rate actually measured, and by Cox et al (1984) on multi-year sea ice. These data are shown in Figure 9 and indicate that the S-2 ice is weaker than the present sea ice. Excellent agreement between the two exponents of strain rate (Frederking's and the current study), however, indicates that the shape of the $\sigma_{1f} - \dot{\varepsilon}_n$ curve for S-2 ice is essentially the same as the $\sigma_{1f} - \dot{\varepsilon}_{1af}$ for the old sea ice. Earlier in this paper it was shown that the average strain rate under confined conditions is less than $\dot{\varepsilon}_n$, though not as much as in the case of unconfined tests. A comparable phenomenon must also have occurred during the confined tests on fresh water ice. Unconfined experiments carried out exhaustively on S-2 ice by Sinha (1981), using the same test machine and specimen size as in the confined tests by Frederking, showed that the specimen strain rates were only 40% of $\dot{\varepsilon}_n$. Frederking's resultant curve, if analysed on the basis of actual strain rates, would therefore have shifted to the lower rates on Figure 9. It is impossible to say, without any measurements, but any such shift would make a better numerical agreement between the two sets of confined test data. This discussion emphasises again the need to make strain measurements directly on specimens during tests, rather than carrying out the analysis on the basis of $\dot{\varepsilon}_n$.

STRESS AND STRAIN AT FAILURE

Failure strain, ε_{1f}, is equal to $\dot{\varepsilon}_{1af}\, t_f$ by definition and it can be shown from Equations (1) and (4) that

$$\varepsilon_{1f} = CP^{-1/p} \left[\frac{\sigma_{1f}}{\sigma_o}\right]^{(1-\theta p)/p} \tag{5a}$$

which on substitution of the values of C, P, p, θ and σ_o gives

$$\varepsilon_{1f} = 5.07 \times 10^{-5}\ (\sigma_{1f})^{2.25} \tag{5b}$$

Equation (5b) is compared with the experimental results in Figure 10. For convenience, unconfined results obtained on pure S-2 ice subjected to a closed-loop controlled constant strain rate (Sinha, 1982) are also shown for comparison. Significant differences between the two sets of results can be seen. Particularly noticeable is the divergence of the two curves as the failure stress or the strain rate and hence the cracking activity increases. It can be shown furthermore using Equations (1) and (4) that

$$\varepsilon_{1f} = CP^{-\theta} \left(\frac{\dot{\varepsilon}_{1af}}{\dot{\varepsilon}_o}\right)^{1-p\theta} \tag{6a}$$

which on substitution of C, P, p, θ and $\dot{\varepsilon}_o$ gives

$$\varepsilon_{1f} = 1.0\ (\dot{\varepsilon}_{1af})^{0.40} \tag{6b}$$

Experimental observations on the dependence of axial upper yield strain on average strain rate is compared with Equation (6b) in Figure 11. Observations on pure S-2 ice under truly constant strain rate is also reproduced in Figure 11 for comparison. In general it takes a strain that is nearly ten times larger in confinement than in unconfined conditions to reach upper yield point. It can be seen that the rate sensitivity of confined failure strain is much greater than that of unconfined strains. The $\varepsilon_{1f} - \dot{\varepsilon}_{1af}$ curve approaches rapidly the curve for unconfined tests as the rate decreases and therefore as the cracking activity decreases.

When tests were conducted under confinement, the lateral or confining stress increased almost proportionately with axial stress during the initial loading period, for example up to about 450 s in Figure 6d. As the axial load increased further with time, the lateral load increased with lower rate. It was noted in all the observations that long and narrow cracks first form with their widths parallel to the direction of the axial load and their long directions parallel to the length of the columnar grains, i.e., parallel to x_3 axis. This observation is similar to what was noted in unconfined creep tests (Gold, 1972) and strength tests (Sinha, 1982) on fresh water columnar-grained S-2 ice. The primary reason for the formation of this type of crack is the two-dimensional nature of deformation in columnar-grained ice when

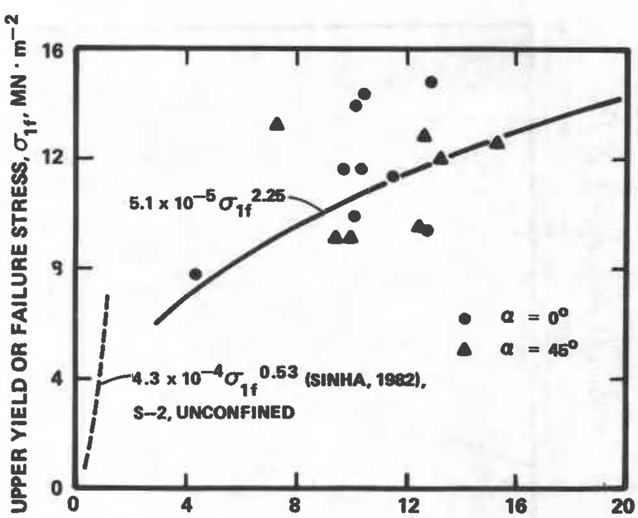

FIG. 10 Relationship between axial failure stress and the corresponding failure strain.

loaded at right angles to the length of the columns. With the continuation of loading, however, the material is forced to deform along the length of the columns, and cracks also start forming at right angles to the columns. Similar observations have also been made in fresh water S-2 ice (Frederking, 1977) during confined tests. This additional mode of deformation introduces a new mechanism of accommodation and lowers the rate of increase in the lateral stress level. Although this subject will be discussed in detail elsewhere, it is appropriate to mention here that the bifurcation in Figure 10, the divergence in Figure 11 and lower rate sensitivity of σ_{1f} may be associated to this mode of deformation. It should be mentioned here that Hirayama et al (1975) also noted the formation of horizontal cracks in fresh water S-2 ice during indentation tests but not until the maximum load was developed.

Figure 12 shows the observed ratio of the lateral stress and the axial stress at upper yield as a function of average strain rate. It also shows the ratio of the lateral strain and axial strain at maximum axial load. The results are rather scattered and, although there appears to be a trend, the effect of strain rate on either the stress ratio or strain ratio cannot be definitely determined. On the average the lateral stress has been found to be 71 ± 14% of the axial failure stress. The average strain ratio is 0.33 ± 0.12. The latter quantity, in fact, gives a measure of the degree of confinement and hence the compliance of the confining frame. Coincidentally this ratio is close to Poisson's ratio of pure polycrystalline ice. Therefore the results obtained here may be applicable to many real life situations where the confinement is provided by the bulk of the ice itself.

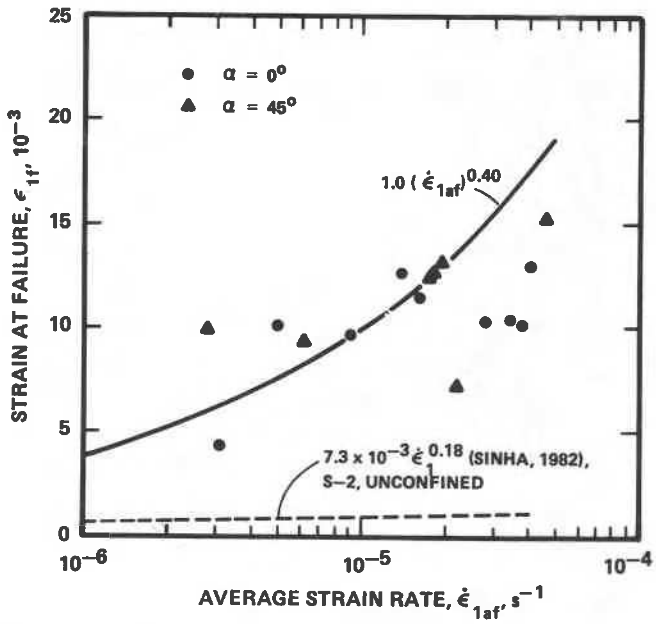

FIG. 11 Dependence of upper axial yield strain on strain rate.

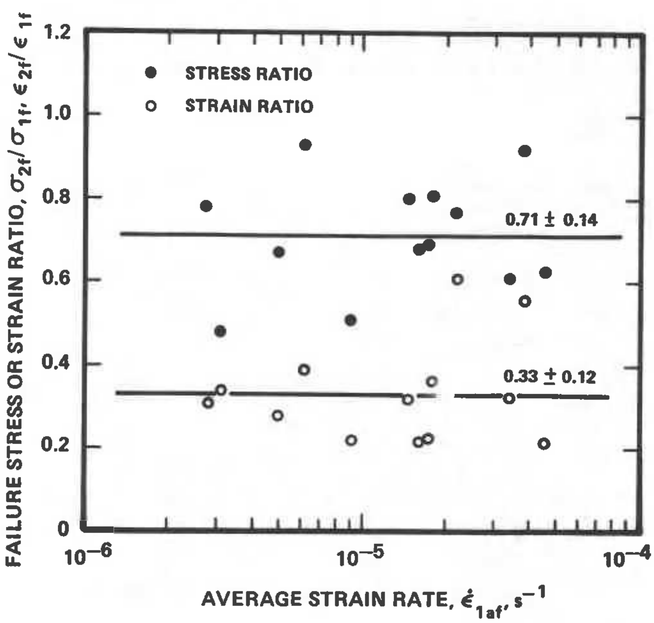

FIG. 12 Strain rate dependence of confining to axial stress ratio and confining to axial strain ratio at upper yield.

CONCLUSIONS

Fully desalinated second-year columnar-grained sea ice with orthotropic texture and fabric has been tested in the field in the High Arctic under confined compressive loading conditions over a wide range of nominally constant cross-head rates at a constant temperature of -10°C. Both stress rate and (measured) strain rate analysis showed that the axial upper yield stress is not affected by the orientation of the load axis with respect to the major crystallographic axis of the grains, where axes of both load and confinement are in the plane at right angles to the long axis of the columnar grains. When compared with the unconfined strength of laboratory-made fresh water columnar-grained ice (as a benchmark), both analyses show that the confinement increases the strength considerably but significantly decreases the rate sensitivity of strength. Both analyses show that the ratio of the confined to the unconfined strength is rate sensitive but the stress rate analysis results in significantly higher ratio than the strain rate analysis. The latter, and more preferable, analysis yielded a ratio of 3.6 to 1.8 in the range of 1×10^{-6} s^{-1} to 1×10^{-4} s^{-1}. Rate sensitivity of the axial failure strain increases considerably by confinement, and the axial failure strains under confinement are about ten times greater than the corresponding values for the unconfined tests. The ratio of the lateral strain at the time of upper yield strain varies significantly, with the average value of 0.33 ± 0.12. The corresponding stress ratio is 0.71 ± 0.14. The most startling observation is that the confined strength of this sea ice is the same as that of fresh water laboratory-made ice tested under almost ideal conditions. This investigation shows that high quality tests can also be performed under field conditions although the test conditions were far from ideal.

ACKNOWLEDGEMENTS

The author is grateful to R.O. Ramseier for the opportunity to participate in the Radarsat Mould Bay Experiment III and for financial support by Atmospheric Environment Service of Environment Canada. He wishes also to express his sincere thanks to C. Bjerkelund, D. Hagen, D. Lapp and L.B. Solar for their assistance in the field and to R. Jerome for his assistance in all the phases of this work including the designing of the subpress. The author particularly acknowledges his wife's full support of this field work even though the birth of their daughter was imminent.

This paper is a contribution from the Division of Building Research, National Research Council of Canada, and is published with the approval of the Director of the Division.

REFERENCES

Blanchet, D. and H. Hamza (1983) Plane-strain compressive strength of first-year Beaufort Sea ice. Proc. 7th POAC 83, Helsinki, Finland, V. 3, p. 84-96.

Cox, G.F.N., J.A. Richter-Menge, W.F. Weeks, M. Mellor and H. Bosworth (1984) Mechanical Properties of Multi-year Sea Ice, Phase I: Test Results, U.S. Army CRREL Report 84-9.

Digby, S.A. (1984) Remote sensing of drained ice areas around breathing holes of ice-inhabiting seals. Canadian Journal of Zoology, 62, p. 1011-14.

Frederking, R.M.W. (1977) Plane-strain compressive strength of columnar-grained and granular-snow ice. J. Glaciology, 18 (80), p. 505-516.

Gold, L.W. (1972) The failure process in columnar-grained ice. National Research Council of Canada, DBR Paper No. 369 (Ph.D. Thesis, McGill University, Montreal).

Hirayama, K., J. Schwarz and H.C. Wu (1975) Ice forces on vertical piles: Indentation and penetration. Proc. 3rd Int. Symp. on Ice Problems, (Int. Assn. Hydraulic Research), Hanover, N.H., p. 429-441.

Holt, B. and S.A. Digby (1984) Processes and imagery of fast first-year sea ice during the melt season. To be published in J.G.R.

Nakawo, M. (1983) Measurements on Air Porosity of Sea Ice. Annals of Glaciology, V. 4, p. 204-208.

Nakawo, M. and N.K. Sinha (1984) A note on brine layer spacing of first-year sea ice. Atmosphere-Ocean, V. 22, No. 2, p. 193-206.

Sinha, N.K. (1977) Dislocation in ice as revealed by etching. Phil. Mag., V. 36, No. 6, p. 1385-1404.

Sinha, N.K. (1981) Rate sensitivity of compressive strength of columnar-grained ice. Experimental Mechanics, V. 21, No. 6, p. 209-218.

Sinha, N.K. (1982) Constant strain- and stress-rate compressive strength of columnar-grained ice. J. Mat. Science, V. 17, No. 3, p. 785-802.

Sinha, N.K. (1983a) Field tests on rate sensitivity of vertical strength and deformation of first-year columnar-grained sea ice. Proc. 7th POAC 83, V. 1, p. 231-242, Technical Research Centre of Finland, Helsinki, Finland.

Sinha, N.K. (1983b) Field Test 1 of compressive strength of first-year sea ice. Annals of Glaciology, 4, p. 253-259.

Sinha, N.K. (1984) Uniaxial compressive strength of first-year and multi-year sea ice. Can. J. Civ. Eng., V. 11, No. 1, p. 82-91.

Timco, G.W. and R. Frederking (1983) Confined Compressive Strength of Sea Ice. Proc. 7th POAC 83, Helsinki, Finland, V. 1, p. 243-253.

Troy, B.E. Jr., J.P. Hollinger, R.O. Ramseier, K.W. Asmus, M.F. Hartman and C.C. Luther (1984) Microwave emission from High Arctic sea ice during freeze-up. To be published in J.G.R.

Weeks, W.F. and A.J. Gow (1978) Preferred crystal orientations in the fast ice along the margins of the Arctic Ocean. Journal of Geophysical Research, 83(C10), p. 5105-5121.

Weeks, W.F. and A.J. Gow (1980) Crystal alignment in the fast ice of Arctic Alaska. Journal of Geophysical Research, 85(C2), p. 1137-1146.

reprinted from

Proceedings of the Fourth International Offshore Mechanics and
Arctic Engineering Symposium – Volume II
Editor: Jin S. Chung
(Book No. I0185B)

published by

THE AMERICAN SOCIETY OF MECHANICAL ENGINEERS
345 East 47th Street, New York, N.Y. 10017
Printed in U.S.A.